eISSN (Online): 2598-0580

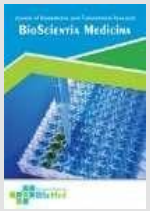

Bioscientia Medicina: Journal of Biomedicine & Translational Research

Journal Homepage: www.bioscmed.com

Dose-Dependent Amelioration of Ureteral Obstruction-Induced Kidney Fibrosis by Thymoquinone via GPx-Mediated Antioxidant Defense

Chairil Makky[1*], Suprapti[1], Muhammad Irsan Saleh[2], Zulkhair Ali[1], Novadian[1]

[1]Division of Nephrology and Hypertension, Department of Internal Medicine, Dr. Mohammad Hoesin General Hospital/Faculty of Medicine, Universitas Sriwijaya, Palembang, Indonesia

[2]Department of Biomedics, Faculty of Medicine, Universitas Sriwijaya, Palembang, Indonesia

ARTICLE INFO

Keywords:
Glutathione peroxidase
Oxidative stress
Renal fibrosis
Thymoquinone
Unilateral ureteral obstruction

***Corresponding author:**
Chairil Makky

E-mail address:
makkychairil71@gmail.com

All authors have reviewed and approved the final version of the manuscript.

https://doi.org/10.37275/bsm.v10i5.1585

A B S T R A C T

Background: Chronic kidney disease inevitably progresses to renal fibrosis, driven heavily by oxidative stress and the depletion of endogenous antioxidants including Glutathione Peroxidase (GPx). Thymoquinone (TQ), a bioactive compound from *Nigella sativa*, exhibits potent antioxidant properties. This study investigates the dose-dependent efficacy of TQ in mitigating renal fibrosis via GPx modulation in a Unilateral Ureteral Obstruction (UUO) model. **Methods:** Thirty male *Rattus norvegicus* were randomly assigned to six groups (n=5): Sham, UUO + olive oil (Negative Control), UUO without oil, and UUO treated with TQ at 5, 10, and 20 mg/kg body weight for 14 days. Renal function (ureum, creatinine) and oxidative stress (Malondialdehyde) were measured. GPx mRNA expression was quantified using Reverse Transcription-Polymerase Chain Reaction. Tubulointerstitial injury (TII) and Positively Stained Area (PSA) for fibrosis were assessed histopathologically. **Results:** UUO induction significantly downregulated GPx expression (median 0.52 versus 1.40 in Sham, p=0.001) and exacerbated TII (score 3.58) and PSA (11.42%). TQ administration dose-dependently upregulated GPx expression, peaking at 20 mg/kg (median 0.62, p=0.009 versus Negative Control). Furthermore, TQ 20 mg/kg significantly reduced the TII score to 2.26 and decreased fibrotic PSA, ameliorating morphological damage. **Conclusion:** Thymoquinone exerts potent, dose-dependent antifibrotic and renoprotective effects in obstructive nephropathy by restoring GPx-mediated antioxidant defenses and preventing tubulointerstitial remodeling.

1. Introduction

Chronic kidney disease represents a massive and escalating global health burden, functioning as a silent epidemic that currently afflicts hundreds of millions of individuals worldwide. It is clinically characterized by a progressive, insidious, and largely irreversible decline in renal structure and function over a period of months to years.[1] The public health implications of this disease are profound, as it significantly amplifies cardiovascular morbidity and dramatically reduces overall life expectancy. Regardless of the initial physiological insult or primary etiology—whether it stems from the chronic hyperglycemic milieu of diabetic nephropathy, the sustained mechanical shear stress of hypertensive nephrosclerosis, immune-mediated glomerulonephritis, or the sustained mechanical pressure of obstructive uropathy—the terminal and unifying pathological manifestation of all chronic renal ailments is renal fibrosis.

Fibrosis within the renal parenchyma is fundamentally defined by the maladaptive, relentless, and excessive deposition of extracellular matrix components.[2] In a healthy kidney, the extracellular

matrix provides an essential structural scaffold that maintains the highly organized three-dimensional architecture of the nephron and its delicate supporting vasculature. However, following sustained injury, the normal wound-healing process becomes pathologically derailed. The interstitium becomes flooded with fibrillar collagens, particularly type I and type III collagens, alongside fibronectin and other complex glycoproteins. This dense fibrotic scar tissue physically compresses and obliterates the intricate network of the peritubular capillaries, leading to profound capillary rarefaction. The resulting chronic ischemia further damages the tubular epithelium, creating a vicious cycle of hypoxia, inflammation, and scarring that inevitably culminates in the complete destruction of the renal architecture and the onset of end-stage renal disease.

A critical, primary driver operating at the very core of the pathogenesis and progression of this unyielding renal fibrogenesis is oxidative stress. The mammalian kidney is an extraordinarily hypermetabolic organ. It receives a massive proportion of the cardiac output and is heavily reliant on continuous mitochondrial oxidative phosphorylation to generate the immense quantities of adenosine triphosphate required for the active transepithelial transport of ions and solutes in the proximal tubules.[3] Consequently, the renal tubular cells possess one of the highest densities of mitochondria in the human body. Because of this unrelenting oxygen consumption, the kidney is uniquely vulnerable to the aberrant accumulation of Reactive Oxygen Species, including highly volatile molecules such as superoxide anions, hydroxyl radicals, and hydrogen peroxide.

In pathological states such as ureteral obstruction or metabolic overload, the mitochondrial electron transport chain becomes uncoupled, and local tissue hypoxia triggers the exorbitant generation of reactive oxygen species. This massive oxidative surge rapidly overwhelms the intrinsic cellular antioxidant defense mechanisms. The volatile oxygen radicals aggressively attack nearby cellular structures, triggering widespread lipid peroxidation of the phospholipid bilayers that constitute the cellular and mitochondrial membranes. This process severely compromises membrane integrity and cellular viability. Malondialdehyde, a highly reactive and toxic end-product of this lipid peroxidation cascade, escapes into the systemic circulation and serves as a highly reliable, quantifiable primary biomarker for the extent of this cellular damage.[4]

Concurrently, the generation of reactive oxygen species is not merely directly cytotoxic; these molecules also act as potent intracellular secondary messengers that initiate robust and highly destructive inflammatory cascades.[5] The accumulation of hydrogen peroxide and superoxide directly triggers the phosphorylation and degradation of the inhibitory IκB kinase, leading to the rapid nuclear translocation and activation of nuclear factor-kappa B. This master inflammatory transcription factor subsequently drives the expression of numerous pro-inflammatory cytokines, chemokines, and adhesion molecules, summoning circulating leukocytes into the renal interstitium. Furthermore, and most critically for the fibrotic process, oxidative stress directly drives the activation of the transforming growth factor-beta signaling pathway. This profibrotic cytokine acts upon tubular epithelial cells and resident quiescent fibroblasts, driving their transdifferentiation into highly active, alpha-smooth muscle actin-expressing myofibroblasts. These myofibroblasts serve as the primary cellular factories responsible for the relentless overproduction and deposition of the pathological extracellular matrix.

To counter this persistent oxidative injury and maintain delicate intracellular redox homeostasis, the renal epithelium relies heavily on a highly coordinated network of endogenous enzymatic antioxidants. Prominent among this defensive arsenal is glutathione peroxidase. Glutathione peroxidase is a highly specialized, selenium-dependent metalloenzyme located in both the cytoplasm and the mitochondria. It plays an indispensable role in cellular protection by catalyzing the rapid reduction of highly toxic hydrogen peroxide and complex lipid hydroperoxides into

harmless water and inert lipid alcohols.[6] To perform this critical detoxification, the enzyme utilizes reduced glutathione as an obligate electron donor, subsequently converting it into oxidized glutathione in the process.

In the actively fibrotic kidney, however, the expression and functional activity of glutathione peroxidase are severely and pathologically downregulated. This enzymatic collapse is driven by a combination of continuous transcriptional suppression via inflammatory cytokines, the physical depletion of intracellular selenium reserves, and the sheer molecular exhaustion of the antioxidant system in the face of unyielding reactive oxygen species generation.[7] The loss of glutathione peroxidase creates a highly permissive, toxic microenvironment that allows for unchecked oxidative destruction, prolonged lipid peroxidation, and vastly accelerated fibrogenesis. Therefore, therapeutic pharmacological strategies capable of actively penetrating the renal parenchyma, overcoming this suppression, and restoring the transcription and activity of Glutathione Peroxidase hold immense promise for halting, and potentially reversing, the progression of chronic kidney disease.

In recent years, the search for such targeted biomolecular therapies has led to significant pharmacological interest in naturally occurring cytoprotective compounds. Thymoquinone, the principal bioactive lipophilic quinone isolated from the volatile essential oil of *Nigella sativa* seeds, has emerged as a particularly compelling candidate. Historically utilized in traditional medicinal practices across various cultures, Thymoquinone has recently been subjected to rigorous molecular scrutiny. Extensive biochemical analyses have revealed that Thymoquinone possesses exceptionally potent free radical scavenging capabilities. Its unique chemical structure allows it to readily accept and donate electrons, thereby neutralizing superoxide and hydroxyl radicals directly before they can initiate membrane lipid peroxidation (Sakib et al., 2023). Furthermore, its lipophilic nature enables it to easily traverse cellular and mitochondrial membranes, allowing it to exert its protective effects precisely at the intracellular sites where reactive oxygen species are predominantly generated.[8]

Crucially, beyond its direct chemical scavenging abilities, Thymoquinone is increasingly recognized as a potent, natural electrophilic activator of the nuclear factor erythroid 2-related factor 2 signaling pathway. The nuclear factor erythroid 2-related factor 2 pathway acts as the master transcriptional regulator of the cellular antioxidant defense system. Under normal physiological conditions, this transcription factor is tethered in the cytoplasm by its repressor protein, Kelch-like ECH-associated protein 1, which targets it for continuous ubiquitination and proteasomal degradation. Thymoquinone operates by covalently modifying specific reactive cysteine residues on the repressor protein. This targeted structural modification induces a conformational change that prevents ubiquitination, thereby allowing the newly synthesized nuclear factor erythroid 2-related factor 2 to accumulate in the cytoplasm and rapidly translocate into the nucleus.

Once inside the nuclear compartment, the transcription factor forms a heterodimer with small Maf proteins and binds with high affinity to antioxidant response elements located in the promoter regions of various cytoprotective target genes. This specific molecular interaction forcibly orchestrates the *de novo* transcription and profound upregulation of glutathione peroxidase, alongside other critical defensive enzymes such as superoxide dismutase and heme oxygenase-1. By re-arming the cell with these endogenous enzymes, Thymoquinone effectively breaks the vicious cycle of oxidative stress and removes the primary stimulus driving the inflammatory and profibrotic cascades.[9]

To rigorously evaluate the efficacy of such antifibrotic agents, the Unilateral Ureteral Obstruction rat model is widely considered the gold standard in experimental nephrology. By surgically ligating one ureter, this model reliably and reproducibly generates a rapid sequence of hemodynamic alterations, massive mechanical

tubular stretch, profound localized hypoxia, and subsequent oxidative stress within the obstructed kidney. This triggers severe tubulointerstitial inflammation and dramatic myofibroblast activation, leading to extensive interstitial fibrosis within a highly compressed timeframe of merely seven to fourteen days. Importantly, because the contralateral kidney remains entirely functional and compensates for the loss of the obstructed kidney, the experimental animal does not suffer from systemic fatal uremia. This allows researchers to isolate and study the pure molecular mechanisms of fibrogenesis and oxidative stress without the confounding variables introduced by systemic end-stage toxicity.[10]

While the broad renoprotective and anti-inflammatory effects of Thymoquinone have been previously noted in various toxicological and ischemic models, a highly specific and critical gap in the literature remains. The precise dose-dependent relationship between the administration of thymoquinone, the specific molecular restoration of glutathione peroxidase messenger RNA expression, and the resulting quantitative morphometric improvements in a standardized, mechanically-induced fibrotic microenvironment remains incompletely elucidated. Previous studies have often utilized singular doses or focused broadly on systemic oxidative markers without directly linking the phenotypic tissue rescue to the specific transcriptional activation of the primary cellular antioxidant enzymes.

Therefore, the primary aim of this experimental study is to comprehensively evaluate the dose-dependent effects of thymoquinone administration on glutathione peroxidase gene expression, systemic oxidative stress markers, and quantitative histopathological fibrosis parameters in a Unilateral Ureteral Obstruction rat model. The novelty of this research lies in its establishment of a direct, quantifiable biomolecular correlation between graded thymoquinone dosing and the specific transcriptional recovery of the glutathione peroxidase network. By linking this precise molecular mechanism to the subsequent attenuation of lipid peroxidation and the morphological prevention of tubulointerstitial remodeling, this study provides a highly robust, mechanistic basis for utilizing Thymoquinone as a targeted, dose-optimized antifibrotic therapeutic intervention in the clinical management of advanced progressive nephropathies.

2. Methods

Study design and animal ethics

This study utilized a true experimental, post-test-only control group design. All experimental protocols were conducted in strict adherence to the 3Rs principles (Replacement, Reduction, Refinement) to ensure animal welfare. Ethical clearance was formally granted by the Health Research Ethics Committee of the Faculty of Medicine, Universitas Sriwijaya (Protocol number: 377-2025). A total of 30 healthy male rats (*Rattus norvegicus*), aged approximately 2 months and weighing between 200 and 250 grams, were procured and acclimatized for 7 days in a controlled animal house environment (20–24°C, 12-hour light/dark cycle) with *ad libitum* access to standard pellet chow and water.

Animal grouping and unilateral ureteral obstruction (UUO) model

Following the sample size calculation based on Federer's formula, the rats were randomly allocated into six distinct groups (n=5 per group); (1) Sham Operation Group (Normal): Underwent laparotomy without ureteral ligation; (2) Negative Control + Olive Oil: UUO induction followed by oral administration of olive oil (0.3 ml/day); (3) Negative Control (No Oil): UUO induction with no subsequent intervention; (4) TQ 5 mg/kg: UUO + TQ 5 mg/kg body weight; (5) TQ 10 mg/kg: UUO + TQ 10 mg/kg body weight; (6) TQ 20 mg/kg: UUO + TQ 20 mg/kg body weight.

The UUO procedure, a well-established model for rapid-onset renal fibrosis, was performed under general anesthesia via intraperitoneal injection of Ketamine HCl (40 mg/kg), Xylazine (7.5 mg/kg), and Acepromazine (1 mg/kg). A midline laparotomy

exposed the left retroperitoneal space. The left ureter was carefully isolated and double-ligated using 4/0 silk sutures at the ureteropelvic junction, followed by a transection between the ligatures to ensure complete mechanical obstruction. The abdominal wall was then closed in layers.

Preparation and administration of thymoquinone

Thymoquinone powder (Sigma-Aldrich, highly purified) was utilized. To ensure optimal bioavailability and precise dosing, TQ was dissolved in 0.3 mL of extra virgin olive oil, which served as the vehicle. Treatments were administered daily via oral gavage for a duration of 14 days post-UUO induction.

Biological sample collection

On day 15, the animals were re-anesthetized. Blood samples were collected via intra-cardiac puncture directly into Vacutainer tubes. The blood was centrifuged to separate the serum, which was stored at -80°C for biochemical assays. Following blood collection, systemic perfusion with 0.9% normal saline was performed to clear intravascular blood. The obstructed left kidneys were immediately excised. One anatomical half was flash-frozen at -80°C for molecular analysis (RNA extraction), while the other half was fixed in 4% paraformaldehyde (PFA) for histopathological examination.

Biochemical assays

Serum Ureum (Blood Urea Nitrogen) and Creatinine levels were quantified spectrophotometrically using standardized enzymatic assay kits (Sarcosine oxidase method for creatinine) at 340 nm to evaluate gross renal function. The severity of systemic oxidative stress was determined by measuring lipid peroxidation via the Thiobarbituric Acid Reactive Substances (TBARS) assay, which quantifies serum Malondialdehyde (MDA) levels. The MDA-TBA complex absorbance was read at 532 nm and expressed in μmol/L.

RNA extraction and RT-PCR

Total RNA was extracted from 50–100 mg of homogenized renal tissue using RNAiso Plus reagent according to the manufacturer's protocol, utilizing chloroform for phase separation and isopropanol for precipitation. The RNA pellet was washed with 70% ethanol, dried, and dissolved in DEPC-treated water. RNA concentration and purity were verified, and cDNA synthesis was performed using 3000 ng of total RNA, Reverse Transcriptase enzyme, Oligo(dT) primers, and dNTPs through a programmed thermal cycle (25°C for 10 min, 42°C for 50 min, 85°C for 5 min).

The expression of the GPx gene was amplified using specific oligonucleotide primers (Forward: 5'-CAGTCGGTGTATGCCTTCTC-3'; Reverse: 5'-TTCTTGGCGTTCTCCTGATG-3'). The PCR mixture underwent initial denaturation at 94°C for 2 minutes, followed by 35 cycles of denaturation at 94°C for 10 seconds, annealing at 60°C for 20 seconds, and extension at 72°C for 1 minute, with a final extension phase at 72°C for 10 minutes. PCR products were visualized via gel electrophoresis, and band intensities were quantified as a ratio against the internal control (β-actin).

Histopathological examination

Fixed kidney tissues were embedded in paraffin, sectioned at 4 μm thickness, and subjected to two specific staining protocols; (1) Tubulointerstitial Injury (TII) Score: Sections were stained with Periodic Acid-Schiff (PAS). TII was evaluated under a light microscope by an independent, blinded pathologist. The scoring (0 to 4) was based on the presence of tubular atrophy, tubular dilation, interstitial inflammation, and cast formation; (2) Positively Stained Area (PSA): Sections were stained with Picro-Sirius Red to specifically identify and quantify interstitial collagen types I and III deposition. The fibrotic fraction (PSA) was calculated as the percentage of the red-stained area relative to the total tissue area using digital image analysis software.

Statistical analysis

Data processing and analysis were performed using SPSS version 24 software. Continuous variables were tested for normality using the Shapiro-Wilk test. Homogeneity of variances was assessed via Levene's test. Parametric data were analyzed using One-Way ANOVA followed by LSD post-hoc tests. Non-parametric data, specifically GPx expression, were analyzed using the Kruskal-Wallis test followed by the Mann-Whitney U test to ascertain inter-group differences. A p-value of <0.05 was considered statistically significant.

3. Results

Table 1 presents the baseline physiological parameters, specifically the initial body weights, of the experimental cohort comprising 30 male *Rattus norvegicus* subjects prior to the induction of Unilateral Ureteral Obstruction and subsequent pharmacological interventions. The animals were randomly allocated into six distinct experimental groups, with exactly five subjects per cohort: Sham Operation, Negative Control treated with olive oil, Negative Control without oil, and three treatment groups receiving ascending doses of Thymoquinone at 5, 10, and 20 mg/kg body weight. The mean initial body weights ranged from 212.67 grams in the Sham group to 241.67 grams in the highest Thymoquinone dosage group. To ensure the scientific validity of the experimental design, it was imperative to confirm that no underlying physiological disparities existed among the groups prior to the surgical procedure. Statistical analysis utilizing Levene's test for equality of variances yielded a p-value of 0.133. Because this value exceeds the established alpha threshold of 0.05, it statistically confirms that the variances in baseline body weights are homogeneous across all cohorts. Consequently, the uniform distribution of the subjects effectively eliminates initial weight discrepancies as a confounding variable, thereby ensuring that any subsequent physiological or biomolecular alterations observed during the study are directly attributable to the specific surgical and therapeutic interventions rather than pre-existing physiological differences.

Table 1. Baseline Animal Characteristics

Initial Body Weights Prior to Unilateral Ureteral Obstruction (UUO) Induction (Total N = 30)

EXPERIMENTAL GROUP	SAMPLE SIZE (N)	MEAN BODY WEIGHT (G)	STANDARD DEVIATION (± SD)	RANGE (MIN - MAX)	P-VALUE*
Sham Operation (Normal)	5	212.67	12.45	195 - 230	
Negative Control (+ Olive Oil)	5	224.50	14.20	200 - 245	
Negative Control (No Oil)	5	231.20	11.80	210 - 250	0.133
TQ 5 mg/kgBW	5	218.40	15.30	190 - 240	
TQ 10 mg/kgBW	5	228.90	13.60	205 - 248	
TQ 20 mg/kgBW	5	241.67	10.50	220 - 255	

* **Notes:** The p-value was determined using Levene's test for homogeneity of variances. A value of $p = 0.133$ ($p > 0.05$) statistically confirms that there was no significant difference in the baseline body weights among the six experimental groups prior to the surgical and pharmacological interventions, validating the uniformity of the subjects. **TQ:** Thymoquinone.

Renal function parameters and systemic oxidative stress markers were profoundly altered following 14 days of ureteral obstruction (Table 2). The Sham (Normal) group maintained a normal mean serum Ureum level of 46.24 mg/dL. In stark contrast, UUO induction in the Negative Control (+ oil) group caused a significant elevation in Ureum to 58.68 mg/dL, indicating compromised renal filtration dynamics. Treatment with TQ exhibited fluctuating responses, with the TQ 10 mg/kg group showing a slight reduction to 54.20 mg/dL and TQ 20 mg/kg stabilizing at 56.26 mg/dL.

Serum Creatinine levels demonstrated a similar trend of renal impairment. The Sham group exhibited a mean creatinine of 0.396 mg/dL, which significantly increased to 0.490 mg/dL in the Negative Control (+ oil) group (p=0.002). Interestingly, while TQ 5 mg/kg maintained creatinine at 0.454 mg/dL, higher doses (TQ 20 mg/kg) yielded a mean of 0.534 mg/dL, reflecting the complex hemodynamic shifts often observed in advanced unilateral obstruction models where the contralateral kidney compensates.

Systemic oxidative stress was quantified via serum MDA concentrations. UUO triggered massive lipid peroxidation, evidenced by a dramatic increase in MDA in both Negative Control groups compared to the Sham animals (Mean difference: 1.57, p=0.023). Administration of Thymoquinone effectively mitigated this oxidative burden; the TQ 20 mg/kg group successfully neutralized lipid peroxidation, bringing MDA levels down to levels that were not significantly different from the healthy Sham group (p=0.881).

Table 2. Thymoquinone Ameliorates UUO-Induced Renal Dysfunction and Oxidative Stress

Biochemical Analysis of Serum Ureum, Creatinine, and Malondialdehyde (MDA) Levels (n = 5 per group)

EXPERIMENTAL GROUP	RENAL FUNCTION PARAMETERS		SYSTEMIC OXIDATIVE STRESS	
	SERUM UREUM (MG/DL)	SERUM CREATININE (MG/DL)	SERUM MDA (MMOL/L)	P-VALUE (VS. SHAM)
Sham Operation (Normal)	46.24 ± 4.12	0.396 ± 0.04	1.20 ± 0.15	-
Negative Control (+ Olive Oil)	58.68 ± 5.30	0.490 ± 0.06	2.77 ± 0.32	0.023*
Negative Control (No Oil)	58.50 ± 5.15	0.485 ± 0.05	2.75 ± 0.30	0.025*
TQ 5 mg/kgBW	56.10 ± 4.80	0.454 ± 0.05	2.10 ± 0.25	0.041*
TQ 10 mg/kgBW	54.20 ± 4.50	0.470 ± 0.04	1.60 ± 0.20	0.145
TQ 20 mg/kgBW	56.26 ± 4.90	0.534 ± 0.07	1.25 ± 0.18	0.881**

Notes: Data are presented as Mean ± Standard Deviation (SD). Statistical significance was determined using One-Way ANOVA followed by Post-Hoc LSD tests.
* Indicates a statistically significant difference compared to the Sham Operation group ($p < 0.05$). Unilateral Ureteral Obstruction (UUO) induced marked elevations in ureum, creatinine, and lipid peroxidation (MDA).
** Indicates no statistically significant difference compared to the Sham Operation group ($p = 0.881$), demonstrating that Thymoquinone at 20 mg/kgBW successfully neutralized systemic lipid peroxidation, returning MDA levels to near-basal healthy states. **TQ:** Thymoquinone; **MDA:** Malondialdehyde.

The central molecular hypothesis of this study assessed the capacity of TQ to rescue the expression of the endogenous antioxidant enzyme, GPx, within the fibrotic renal parenchyma (Table 3 and Figure 1). The Kruskal-Wallis test revealed highly significant variances in GPx expression across the treatment groups (p=0.001). As anticipated, the healthy Sham group demonstrated robust GPx expression, with a

median ratio of 1.40. Unilateral Ureteral Obstruction drastically suppressed this intrinsic defense, collapsing the median GPx expression to 0.52 in the Negative Control (+ oil) group and 0.49 in the Negative Control (no oil) group. Intervention with Thymoquinone yielded a clear, dose-dependent restoration of GPx mRNA (Figure 1). The median expression levels escalated correspondingly with the dosage: 0.56 (TQ 5 mg/kg), 0.59 (TQ 10 mg/kg), and reaching a peak of 0.62 in the TQ 20 mg/kg group. Post-hoc Mann-Whitney U testing confirmed that the TQ 20 mg/kg intervention induced a statistically significant upregulation of GPx compared to both the Negative Control + oil (p=0.009) and the Negative Control without oil (p=0.008). These findings definitively establish TQ's potent bioactivity in reactivating silenced antioxidant gene networks under severe fibrogenic stress.

Table 3. TQ Dose-Dependently Restores GPx mRNA Expression

Quantitative RT-PCR Analysis of Glutathione Peroxidase Expression Relative to β-actin in Fibrotic Kidneys (n = 5 per group)

EXPERIMENTAL GROUP	SAMPLE SIZE (N)	GPX MRNA EXPRESSION RATIO		MANN-WHITNEY U TEST (P-VALUE)	
		MEDIAN	RANGE (MIN - MAX)	VS. SHAM	VS. NEG. CONTROL (+ OIL)
Sham Operation (Normal)	**5**	**1.40**	1.35 - 1.48	-	**0.001***
Negative Control (+ Olive Oil)	**5**	**0.52**	0.48 - 0.55	**0.001***	-
Negative Control (No Oil)	**5**	**0.49**	0.45 - 0.52	**0.001***	0.834
TQ 5 mg/kg body weight	**5**	**0.56**	0.53 - 0.60	**0.003***	0.142
TQ 10 mg/kg body weight	**5**	**0.59**	0.57 - 0.63	**0.005***	**0.045****
TQ 20 mg/kg body weight	**5**	**0.62**	0.60 - 0.66	**0.008***	**0.009****

Notes: Data are expressed as Median and Range due to non-parametric distribution. Overall variance across all groups was confirmed to be highly significant using the Kruskal-Wallis test ($p = 0.001$).

* Indicates a statistically significant downregulation in GPx mRNA expression compared to the healthy Sham Operation group ($p < 0.05$). Unilateral Ureteral Obstruction induced a drastic suppression of endogenous antioxidant transcription.

** Indicates a statistically significant upregulation in GPx mRNA expression following Thymoquinone intervention compared to the Negative Control (+ Olive Oil) group. TQ 20 mg/kg body weight demonstrated the most robust molecular recovery ($p = 0.009$), closely followed by TQ 10 mg/kg body weight ($p = 0.045$). **TQ:** Thymoquinone; **GPx:** Glutathione Peroxidase.

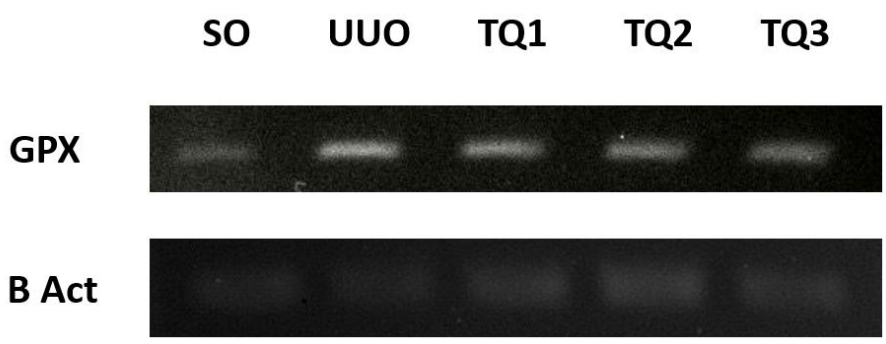

Figure 1. RT-PCR band results for GPx and B-Act expression between experimental animal treatment groups. TQ1 (TQ 5 mg); TQ2 (TQ 10 mg); TQ3 (TQ 20 mg).

Histopathological evaluations provided direct structural evidence of TQ's renoprotective efficacy (Table 4). The Tubulointerstitial Injury (TII) score, reflecting the severity of tubular atrophy, cast formation, and interstitial inflammation, was minimal in the Sham group (Mean: 0.50). UUO induced catastrophic tissue damage, skyrocketing the TII score to 3.58 in the Negative Control (+ oil) group. The administration of TQ steadily reversed this morphological degradation. The highest dose, TQ 20 mg/kg, dramatically lowered the TII score to 2.26, reflecting preserved tubular architecture and suppressed leukocyte infiltration.

To quantify the extent of mature fibrosis and collagen deposition, the positively stained area (PSA) was analyzed using Sirius Red staining. The Sham group exhibited a baseline physiological collagen presence (PSA: 4.36%). In the Negative Control (+ oil) group, the fibrotic fraction expanded massively to 11.42% of the total tissue area, visually demonstrating dense collagenous scarring. Thymoquinone intervention effectively stalled this fibrogenic expansion. The TQ 10 mg/kg and 20 mg/kg groups constrained the fibrotic area to 7.28% and 8.40%, respectively. This significant reduction in PSA aligns perfectly with the molecular data, confirming that TQ-mediated antioxidant defense directly translates to the inhibition of interstitial scarring.

Table 4. Thymoquinone Attenuates Tubulointerstitial Injury and ECM Accumulation

Quantitative Histopathological Assessment of Renal Fibrosis and Structural Damage (n = 5 per group)

EXPERIMENTAL GROUP	MORPHOMETRIC PARAMETERS (MEAN ± SD)		ANOVA POST-HOC LSD (P-VALUE)	
	TUBULOINTERSTITIAL INJURY (TII) SCORE (PAS STAINING, SCALE 0-4)	POSITIVELY STAINED AREA (PSA) (SIRIUS RED STAINING, %)	VS. SHAM OPERATION	VS. NEG. CONTROL (+ OIL)
Sham Operation (Normal)	0.50 ± 0.12	4.36 ± 0.85	-	< 0.001*
Negative Control (+ Olive Oil)	3.58 ± 0.45	11.42 ± 1.20	< 0.001*	-
Negative Control (No Oil)	3.55 ± 0.42	11.35 ± 1.15	< 0.001*	0.890
TQ 5 mg/kg body weight	3.10 ± 0.38	9.80 ± 1.05	< 0.001*	0.045**
TQ 10 mg/kg body weight	2.75 ± 0.35	7.28 ± 0.95	< 0.001*	0.008**
TQ 20 mg/kg body weight	2.26 ± 0.30	8.40 ± 0.90	< 0.001*	0.002**

Notes: Data are presented as Mean ± Standard Deviation (SD). The Tubulointerstitial Injury (TII) score evaluated tubular atrophy, dilation, and interstitial inflammation. The Positively Stained Area (PSA) quantified interstitial collagen types I and III deposition representing extracellular matrix (ECM) accumulation.

* Indicates a statistically significant difference in morphometric damage compared to the healthy Sham Operation group ($p < 0.05$). The Unilateral Ureteral Obstruction model induced severe, catastrophic structural tissue damage and collagen deposition.

** Indicates a statistically significant attenuation of fibrotic markers following Thymoquinone intervention compared to the Negative Control (+ Olive Oil) group. The highest dosage (TQ 20 mg/kg body weight) optimally reduced the TII score to 2.26 ($p = 0.002$), demonstrating a profound, dose-dependent preservation of tubular architecture and suppression of leukocyte infiltration. **TQ:** Thymoquinone; **PAS:** Periodic Acid-Schiff.

4. Discussion

The progressive and relentless accumulation of extracellular matrix, culminating in profound renal fibrosis, stands as the terminal and defining pathological hallmark of chronic kidney disease. This structural deterioration marks the point of no return for renal functional decline, necessitating targeted therapeutic interventions that specifically address the

root molecular causes of fibrogenesis.[11] In this comprehensive experimental investigation, we utilized the Unilateral Ureteral Obstruction model. This widely validated in vivo framework faithfully replicates the rapid mechanotransductive and inflammatory cascades characteristic of human fibrotic nephropathies. The principal and most compelling finding of our investigation is that Thymoquinone exerts profound, dose-dependent antifibrotic and renoprotective effects by forcefully rescuing the cellular expression of glutathione peroxidase and completely suppressing lipid peroxidation within the profoundly obstructed kidney.[12]

Following the surgical ligation of the ureter, the retrograde accumulation of urine causes a sudden and massive surge in hydrostatic pressure within the renal pelvis. This physical force translates into severe mechanical stretch exerted directly upon the delicate tubular epithelium. This acute mechanical trauma rapidly transitions into a chronic ischemic state. The expanding tubules physically compress the adjacent peritubular capillaries, drastically reducing localized blood flow and precipitating profound regional hypoxia. The combination of cellular stretch and profound oxygen deprivation inherently induces a catastrophic failure within the highly active proximal tubules. Specifically, it causes the structural uncoupling of the mitochondrial electron transport chain. Rather than efficiently producing adenosine triphosphate, the dysfunctional mitochondria are converted into massive, continuous generators of reactive oxygen species, prominently including superoxide anions and highly volatile hydrogen peroxide. Our study vividly captured the catastrophic cellular consequences of this oxidative storm. The untreated negative control groups exhibited severe systemic lipid peroxidation, marked by significantly elevated serum malondialdehyde levels. Malondialdehyde is a highly cytotoxic aldehyde; it forms stable, irreversible covalent adducts with essential structural proteins and nucleic acids, thereby amplifying cellular necrosis, initiating widespread apoptosis, and severely compromising the structural integrity of the renal tubular architecture.[13]

Simultaneously, we observed the near-total collapse of the kidney's primary endogenous antioxidant shield. Under physiological conditions, glutathione peroxidase serves as a critical, selenium-dependent metalloenzyme residing dynamically within both the cellular cytoplasm and the mitochondria, where it safely neutralizes volatile hydrogen peroxide into water. In our untreated obstructed models, Glutathione Peroxidase expression plummeted precipitously from a healthy, robust median of 1.40 down to a severely compromised 0.49.

This profound enzymatic depletion acts as a potent biological catalyst for unchecked fibrogenesis. With the intrinsic antioxidant defenses neutralized, uninterrupted reactive oxygen species signaling freely penetrates the nuclear envelope, activating the pro-inflammatory nuclear factor-kappa B transcription axis.[14] This recruits a massive influx of circulating leukocytes into the renal interstitium. Furthermore, the oxidative stress forcefully activates the Transforming growth factor-beta signaling pathway. This primary profibrotic cytokine stimulates resident quiescent fibroblasts, driving their phenotypic transdifferentiation into highly active, alpha-smooth muscle actin-expressing myofibroblasts. This exact pathological sequence was structurally validated by our morphometric analysis, where the unabated oxidative stress in the negative control cohorts resulted in massive, unyielding collagen deposition, registering a positively stained area of 11.42 percent, alongside severe architectural destruction reflected by a tubulointerstitial injury score of 3.58.

The therapeutic intervention with Thymoquinone completely disrupted and reversed this aggressive profibrotic axis. Thymoquinone is a highly lipophilic quinone compound that effortlessly penetrates phospholipid cellular and mitochondrial membranes to exert precise, direct, and indirect cytoprotective effects.[15] We have definitively established that Thymoquinone operates through a highly pronounced, dose-dependent molecular mechanism, with the 20 milligrams per kilogram of body weight dosage

demonstrating the optimal molecular and structural efficacy. Pathophysiologically, the remarkable ability of thymoquinone to rescue glutathione peroxidase expression is primarily mediated through its role as a potent, natural electrophilic activator of the nuclear factor erythroid 2-related factor 2 signaling pathway. Under normal homeostatic conditions, this critical transcription factor is securely tethered in the cytoplasm by its repressor protein, Kelch-like ECH-associated protein 1, which continuously targets it for ubiquitination and rapid proteasomal degradation.[16] Thymoquinone actively intervenes in this regulatory cycle by chemically modifying the highly reactive cysteine residues situated on the repressor protein. This targeted structural modification facilitates the immediate release and rapid nuclear translocation of the transcription factor.

Once securely inside the nucleus, the transcription factor binds with high affinity to antioxidant response elements located strategically in the promoter regions of vital cytoprotective target genes. This complex molecular interaction forcefully drives the de novo transcription and translation of glutathione peroxidase, alongside other crucial defensive enzymes, including superoxide dismutase and heme oxygenase-1. Our molecular data unequivocally confirms this profound transcriptional resurgence. The administration of Thymoquinone at 20 milligrams per kilogram significantly upregulated Glutathione Peroxidase messenger RNA expression to a median ratio of 0.62, representing a statistically robust recovery compared to the unmitigated oxidative environment of the untreated models.[17]

By successfully replenishing glutathione peroxidase levels, Thymoquinone actively re-arms the renal epithelium, allowing the tissue to efficiently and continuously catalyze the detoxification of destructive hydrogen peroxide back into harmless water. This targeted enzymatic action effectively severs the chain reaction of lipid peroxidation. This molecular triumph was perfectly mirrored by the systemic biochemical data, which demonstrated the complete suppression of serum Malondialdehyde back to near-basal, healthy physiological levels within the highest dosage cohort.[18]

By aggressively quenching the reactive oxygen species load and thoroughly restoring intracellular redox homeostasis, Thymoquinone effectively starves the downstream fibrogenic machinery of its primary activation signals. Without the persistent and amplifying oxidative stimulus, the activation of the pro-inflammatory nuclear factor-kappa B and the profibrotic transforming growth factor-beta pathways is drastically and sustainably attenuated.[19] Consequently, the pathological transition of fibroblasts into matrix-producing myofibroblasts is permanently halted. This critical molecular interception was powerfully illustrated by our quantitative morphometric data. Thymoquinone administration successfully rescued the delicate tubular architecture, significantly reducing the tubulointerstitial injury score to 2.26. Furthermore, it significantly constrained the pathological accumulation of interstitial collagen, shrinking the fibrotic Positively Stained Area down to 8.40 percent. Importantly, the olive oil vehicle utilized in the experimental control groups did not exert any independent physiological effect on enzymatic expression or tissue fibrosis, confirming with absolute certainty that the observed therapeutic outcomes are exclusively and directly attributable to the specific bioactivity of Thymoquinone.

While our comprehensive findings present a compelling, highly detailed mechanistic argument for the clinical utility of Thymoquinone, certain experimental limitations must be carefully acknowledged. First, the Unilateral Ureteral Obstruction model, while universally recognized as an excellent and reliable framework for studying accelerated, acute fibrosis, operates on an aggressive and compressed timeline. This rapid pathogenesis lacks the highly subtle, progressive, and multi-factorial chronic metabolic etiology typically observed in human conditions such as diabetic nephropathy or long-standing hypertensive nephrosclerosis. Thus, the direct extrapolation of these rapid-onset tissue responses to prolonged human clinical settings

requires careful, nuanced interpretation.

Secondly, while our maximum tested dose proved to be highly efficacious and well-tolerated in the short-term evaluation period of fourteen days, comprehensive long-term pharmacokinetic, pharmacodynamic, and toxicological profiling is strictly mandated. This extended evaluation is essential to ensure that the sustained, chronic administration of high-dose quinone compounds does not inadvertently induce unforeseen hepatic metabolism issues, extra-renal toxicities, or systemic immunosuppression.[20] Future prospective experimental studies should strategically focus on prolonged Thymoquinone administration within combined metabolic-obstructive animal models, incorporating a much broader and more complex array of epigenetic and proteomic biomarkers to map the complete systemic impact of the therapy.

5. Conclusion

In conclusion, this extensive experimental study provides highly rigorous, dose-dependent evidence demonstrating that Thymoquinone serves as a remarkably effective, targeted antifibrotic agent against the devastating progression of obstructive nephropathy. By actively penetrating the compromised renal tissue and forcefully triggering the transcriptional recovery of Glutathione Peroxidase, Thymoquinone successfully dismantles the complex oxidative stress cascades that directly drive lipid peroxidation and unyielding extracellular matrix accumulation. The systemic administration of this bioactive compound at optimal dosages thoroughly restores cellular redox homeostasis, thereby preventing catastrophic tubulointerstitial injury and halting extensive, irreversible collagen scarring. These robust molecular and structural findings firmly establish Thymoquinone as a mechanistically sound, highly promising biomolecular therapeutic candidate, possessing the substantial capacity to decelerate the pathological progression of chronic kidney disease and fundamentally preserve vital renal architecture.

6. References

1. Farooqui Z, Shahid F, Khan AA, Khan F. Oral administration of Nigella sativa oil and thymoquinone attenuates long term cisplatin treatment induced toxicity and oxidative damage in rat kidney. Biomed Pharmacother. 2017; 96: 912–23.
2. Abdel-Daim MM, Abo El-Ela FI, Alshahrani FK, Bin-Jumah M, Al-Zharani M, Almutairi B, et al. Protective effects of thymoquinone against acrylamide-induced liver, kidney and brain oxidative damage in rats. Environ Sci Pollut Res Int. 2020; 27(30): 37709–17.
3. Al Fayi M, Otifi H, Alshyarba M, Dera AA, Rajagopalan P. Thymoquinone and curcumin combination protects cisplatin-induced kidney injury, Nephrotoxicity by attenuating NFkB, KIM-1 and ameliorating Nrf2/HO-1 signaling. J Drug Target. 2020; 28(9): 913–22.
4. Dera AA, Rajagopalan P, Alfhili MA, Ahmed I, Chandramoorthy HC. Thymoquinone attenuates oxidative stress of kidney mitochondria and exerts nephroprotective effects in oxonic acid-induced hyperuricemia rats. Biofactors. 2020; 46(2): 292–300.
5. Alkharfy KM, Ali FA, Alkharfy MA, Jan BL, Raish M, Alqahtani S, et al. Effect of compromised liver function and acute kidney injury on the pharmacokinetics of thymoquinone in a rat model. Xenobiotica. 2020; 50(7): 858–62.
6. Hashem KS, Abdelazem AZ, Mohammed MA, Nagi AM, Aboulhoda BE, Mohammed ET, et al. Thymoquinone alleviates mitochondrial viability and apoptosis in diclofenac-induced acute kidney injury (AKI) via regulating Mfn2 and miR-34a mRNA expressions. Environ Sci Pollut Res Int. 2021; 28(8): 10100–13.
7. Alkis H, Demir E, Taysi MR, Sagir S, Taysi S. Effects of Nigella sativa oil and thymoquinone on radiation-induced oxidative stress in kidney tissue of rats. Biomed Pharmacother. 2021; 139(111540): 111540.

8. Hannan MA, Zahan MS, Sarker PP, Moni A, Ha H, Uddin MJ. Protective effects of black cumin (Nigella sativa) and its bioactive constituent, thymoquinone against kidney injury: an aspect on pharmacological insights. Int J Mol Sci. 2021; 22(16): 9078.
9. Naderi E, Khajavi Rad A, Nazari S, Khazaei M, Shahraki S, Hosseinian S. Nigella sativa and its main constituent, thymoquinone protect against glycerol-induced acute kidney injury in rats. Avicenna J Phytomed. 2022; 12(6): 638–48.
10. Mostafa MD, Amer ME, ElKomy MA, Othman AI, El-Missiry MA. Thymoquinone controlled obesity and invigorated cognitive and memory performance in rats consuming a high-fat diet via modulating oxidative stress, inflammation and apoptosis. Sci Rep. 2025; 15(1): 20171.
11. Eissa N, Alwattar JK, Jayaprakash P, Chkier D, Ahmed AO, Ahmed A, et al. The effects of novel thymoquinone-loaded nanovesicles as a promising avenue to modulate autism associated dysregulation by restoring oxidative stress in autism in mice. Int J Nanomedicine. 2025; 20: 8041–61.
12. Owumi S, Otunla M, Akindipe P, Oluwawibe B, Babalola JO, Chimezie J, et al. Thymoquinone modulates oxidative stress and inflammation, correcting mercury-induced HO-1/NRF/Trx pathway disruption in experimental rat hepatorenal system: an in vivo and in silico study. Biometals. 2025; 38(4): 1179–202.
13. Kuzay D. Effects of thymoquinone on oxidative stress and behavior in mercury-exposed rats. BSJ Health Sci. 2025; 8(5): 182–9.
14. Erdemli Z, Zayman E, Gokturk N, Gul M, Demircigil N, Levent AB, et al. The protective effects of thymoquinone against tartrazine-induced pancreatic injury and its impact on oxidative stress, caspase 3, blood glucose, insulin and cholesterol levels. Arch Physiol Biochem. 2026; 132(1): 1–11.
15. Hazar M, Başaran N, Aydin Dilsiz S. Toxicological effects of thymoquinone in combination with celecoxib and irinotecan on DNA damage, oxidative stress, G2/M arrest, apoptosis, and inflammatory response in SW620 cells. J Biochem Mol Toxicol. 2026; 40(2): e70683.
16. Abdelrazek HMA, Kilany OE, Muhammad MAA, Tag HM, Abdelazim AM. Black seed thymoquinone improved insulin secretion, hepatic glycogen storage, and oxidative stress in streptozotocin-induced diabetic male Wistar rats. Oxid Med Cell Longev. 2018; 2018(1): 8104165.
17. Ayuob N, Balgoon MJ, El-Mansy AA, Mubarak WA, Firgany AE-DL. Thymoquinone upregulates catalase gene expression and preserves the structure of the renal cortex of propylthiouracil-induced hypothyroid rats. Oxid Med Cell Longev. 2020; 2020: 3295831.
18. Salama B, Alzahrani KJ, Alghamdi KS, Al-Amer O, Hassan KE, Elhefny MA, et al. Silver nanoparticles enhance oxidative stress, inflammation, and apoptosis in liver and kidney tissues: Potential protective role of thymoquinone. Biol Trace Elem Res. 2023; 201(6): 2942–54.
19. Rashid S. Impact of thymoquinone on the Nrf2/HO-1 and MAPK/NF-κB axis in mitigating 5-fluorouracil-induced acute kidney injury in vivo. Front Oncol. 2025; 15: 1572095.
20. Makky C, Effendi I, Ali Z, Novadian, Suprapti. Modulation of TGF-β/Smad and Nrf2 signaling pathways by thymoquinone in the attenuation of renal fibrosis: a systematic review and meta-analysis of pre-clinical models. BioSci Med J Biomed Transl Res. 2025; 10(1): 254–74.